Proc. NIPR Symp. Upper Atmos. Phys., 5, 60–69, 1992

PRECIPITATION PATTERN OF ELECTRONS AND PROTONS AT THE ONSET OF AURORAL SUBSTORMS

Rumi NAKAMURA[1] and GADC group[2]

[1] *National Institute of Polar Research, 9–10, Kaga 1-chome, Itabashi-ku, Tokyo 173*
[2] *Department of Earth and Planetary Physics, Faculty of Science, University of Tokyo, 3–1, Hongo 7-chome, Bunkyo-ku, Tokyo 113*

Abstract: Using magnetically conjugate data from DMSP and ground all-sky TV instruments, temporal change in latitudinal structure of electron and proton precipitation is examined for the poleward expansion onsets of aurora during two successive DMSP passes on January 17, 1986. Electron precipitation just before an onset consisted of cold BPS precipitation with an inverted-V at its equatorward boundary, but no detectable CPS at lower latitude. Poleward expansion started from an auroral arc which corresponded to an inverted-V at the BPS equatorward boundary. During an expansion, when multiple inveretd-V were distributed in BPS, intense CPS electron precipitation was observed at lower latitude. This CPS precipitation was associated with the equatorward expansion of aurora during the recovery of the previous auroral activation. It is suggested that the CPS is not merely a stable precipitation, but rather consists of electrons which are accelerated and injected associated with the substorm. As for the ion precipitation, its dependence on the auroral expansion was significantly different with respect to the latitude. At latitudes higher than the BPS equatorward boundary, energetic ion precipitation intensified drastically associated with the auroral expansion, and the region of strongest ion precipitation was collocated at that of strongest electron precipitation. At lower latitude, energetic ions are rather permanent components which expanded in latitudinal width but did not intensify significantly associated with the expansion. The high latitude ion would consist mainly of ions which are accelerated at the substorm onset region together with electrons, whereas the acceleration of the low latitude ions would be maintained with larger temporal scale than a substorm expansion.

1. Introduction

Precipitating particles observed by polar orbiting satellites have been used to specify the magnetospheric particle population. It was shown that the night side auroral oval population consists of structured electron precipitation (referred to as BPS), which produces discrete aurora, and uniform electron precipitation (referred to as CPS), which produces diffuse aurora (LUI and ANGER, 1973). In response to substorms, the BPS exhibits dynamical change in average energy, intensity, as well as location, while the CPS is relatively stable and experiences uniform increase and decrease in intensity and average energy (WINNINGHAM *et al.*, 1975).

Relationship between CPS/BPS precipitation and the region of its origin in the magnetosphere is not yet well understood (FELDSTEIN and GALPERIN, 1985). LUI *et al.* (1977) suggested that the CPS connects to the central plasma sheet.

LYONS and EVANS (1984) have shown that electron precipitations with sufficient energy flux to produce discrete aurora is generally associated with proton precipitation, and they suggested that discrete aurora might be mapped along the outer boundary of the plasma sheet into the tail current sheet.

The main purpose of this study is to examine temporal change in latitudinal profile of both electron and proton precipitation associated with the poleward expansion of aurora. One of the difficulty in satellite study is that the revolution period of a polar orbiting satellite is too long compared with the time scale of a substorm. In this study, we examined simultaneous ground auroral data of high temporal and spatial resolution when the DMSP satellite traversed the field of view of the ground camera. This procedure allows us to discuss the temporal evolution of precipitating pattern. We present two cases of particle and auroral observations on January 17, 1986, when the satellite passed over the auroral zone just before and after the onset of local expansions of aurora in the premidnight sector.

The particle data used in this study were obtained by the DMSP F7 low-altitude (840 km) polar orbiting satellite, which measured precipitating electrons and ions with energies between 30 eV and 30 keV. Detailed descriptions of the satellite and the particle measurement are given in HARDY *et al.* (1984). The auroral data were taken at Shamattawa (geographic: 55.9°N, 267.9°E; geomagnetic: 67.8°N, 330.1°E) and Fort Smith (geographic: 60.0°N, 248.1°E; geomagnetic: 68.2°N, 299.5°E) during the Global Aurora Dynamics Campaign (GADC) period (OGUTI *et al.*, 1988).

2. Analysis of Observations

2.1. Before an onset

Figure 1a shows auroral data at Shamattawa (SHM) from 0445UT on January 17, 1986, including the period when the DMSP was within the field of view of the all-sky TV camera. During the period, SHM was located in the premidnight sector (~22 MLT). The DMSP satellite passed from the north to the south as is shown in the all-sky image of 045820UT. The bottom panel shows the meridian plot of the all-sky TV data from 0440UT to 0540UT. Brightening and a slightly southward motion of a discrete auroral arc at ~69° started at 0456UT. This was followed by a sudden activation and a poleward expansion of the aurora at 0508UT. While the discrete auroral region expanded farther northward until ~0530UT, diffuse auroral region expanded gradually southward to ~68°. The DMSP satellite passed the discrete auroral region just after the brightening, between 045820UT and 045840UT; *i.e.* before the poleward expansion onset. Particle data from DMSP F7 during the period is compared with the all-sky TV auroral data in Fig. 2a. The top four panels show the spectrums and total flux (J_E for the energy flux and J_N for the number flux) for the ions and electrons. The second panel from the bottom shows the distance between the satellite foot point and the zenith of SHM calculated at an altitude of 110 km. The bottom panel shows relative luminosity of aurora at the foot points of DMSP field lines which traversed the field of view of the all-sky TV camera at SHM from north to south. It therefore represents the expected

auroral luminosity which would be produced by the precipitation detected by DMSP. The luminosity is plotted with 256 levels in logarithmic scale with an arbitrary scale. The luminosity level detected by a fish-eyed lens has negative dependence on the zenith angle of the observation point, and so does the background noise level. For this particular plot the background noise level was chosen between 135 and 145 depending on the zenith angle. The sharp peak designated with the letter S in the panel is the light from a star.

The electron spectrogram from 045743UT (71.7° magnetic latitude) to 045831UT (69.3°) shows a relatively weak and cold precipitation with maximum energy flux of <0.1 erg/cm^2/str/sec and maximum average energy of <800 eV. This electron precipitation is comparable to that for the quiet BPS reported by WINNINGHAM *et al.* (1975). The ion also shows a weak precipitation with energy flux of <0.01 erg/cm^2/str/sec before 045831UT. At the equatorward boundary of the quiet BPS region, electron spectrum hardened to an average energy to 1.8 keV between 045831UT (69.3°) and 045836UT (68.9°). This precipitation was an inverted-V (FRANK and ACKERSON, 1971) and was associated with the discrete aurora of SHM shown in the bottom panel. The ion precipitation was also significantly enhanced at the region of the discrete aurora more than 10 times with average energy greater than 10 keV. Equatorward boundary of BPS, which corresponds to the discrete auroral precipitation, was 68.9° for this event. Note that at the lower latitude of this discrete aurora, energy flux was less than 0.001 erg/cm^2/str/sec and there was no detectable CPS electron precipitation. The lack of CPS precipitation is also confirmed from the relative luminosity level that was around the noise level (bottom plot) and from the meridian plot of aurora (Fig. 1a) that shows no diffuse aurora below the latitude of the discrete aurora. As for the ions, the region of enhanced precipitation can be seen until 045850UT (68.2°). During this period, average energy increased with decreasing latitude to 17 keV. This can be identified in the enlarging difference between the energy flux profile and the number flux profile in the second plot, which present the average energy. Such latitudinal relationship has been pointed out as due to an adiabatic compression of the plasma sheet expected from a steady convection electric field (*e.g.*, HARDY *et al.*, 1989). The discrete auroral arc identified from electron precipitation and auroral image was located at the poleward boundary of this ion precipitation region, which is consistent with other satellite particle observations (*e.g.*, LYONS *et al.*, 1988). It should be noted that the poleward expansion started from this particular discrete aurora which was located at the quatorward boundary of the electron BPS precipitation and therefore at the poleward boundary of the enhanced ion precipitation.

2.2. *After an onset*

The next DMSP orbit on January 17 passed the field of view from Fort Smith (FSM) at ~0638UT. Figure 1b shows the auroral data at FSM from 0610UT on January 17, 1986 in the same format as Fig. 1a. During this period, FSM was located in the premidnight sector (~22 MLT). The meridian plot between 0610UT and 0700UT shows that a discrete aurora at ~69° activated and expanded poleward from 0617UT. This activation was associated with a passage of a westward traveling

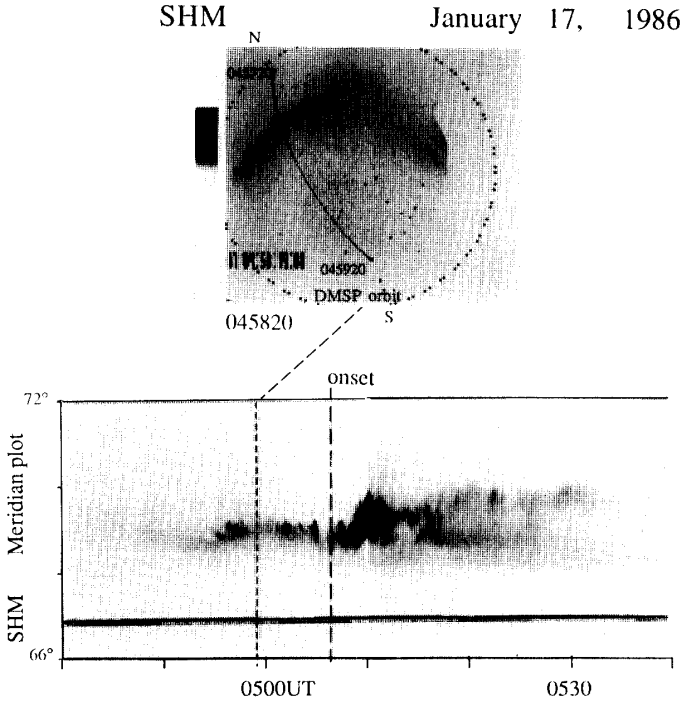

Fig. 1a. Auroral data at Shamattawa (SHM) on January 17, 1986. The upper panel shows an all-sky TV image at 045820UT. The DMSP orbit track is superimposed on the image. The bottom panel is a meridian plot of the aurora from 0440UT to 0540UT Both panels are given here in negative images.

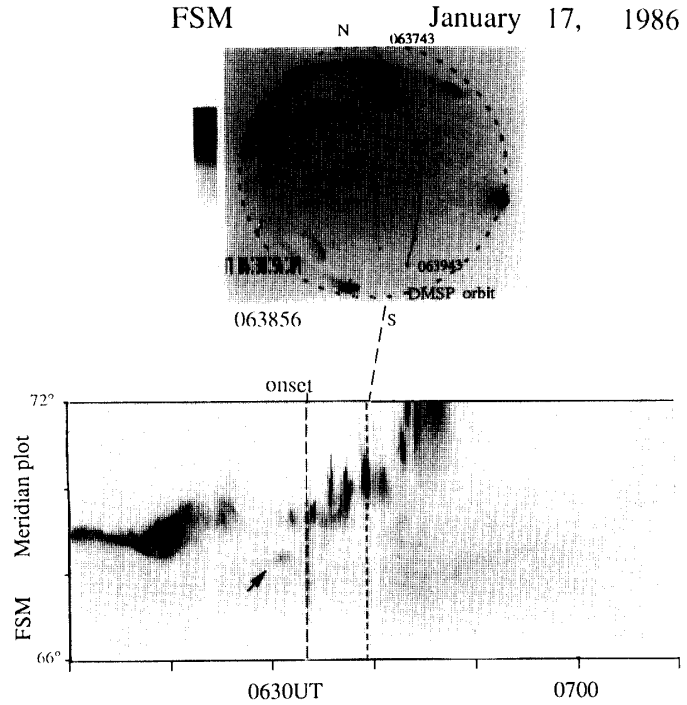

Fig. 1b Auroral data at Fort Smith (FSM) from 0610UT to 0710UT on January 17, 1986 in the same format as Fig. 1a.

surge, which was confirmed with the TV data from FSM (not shown). The auroral activity calmed down by ~0633UT. During this recovery phase, auroral structures moved southward from ~69.5° (0626UT) to ~68.5° (0632UT) and after an intensification (indicated by the arrow) it turned into diffuse aurora. The next auroral

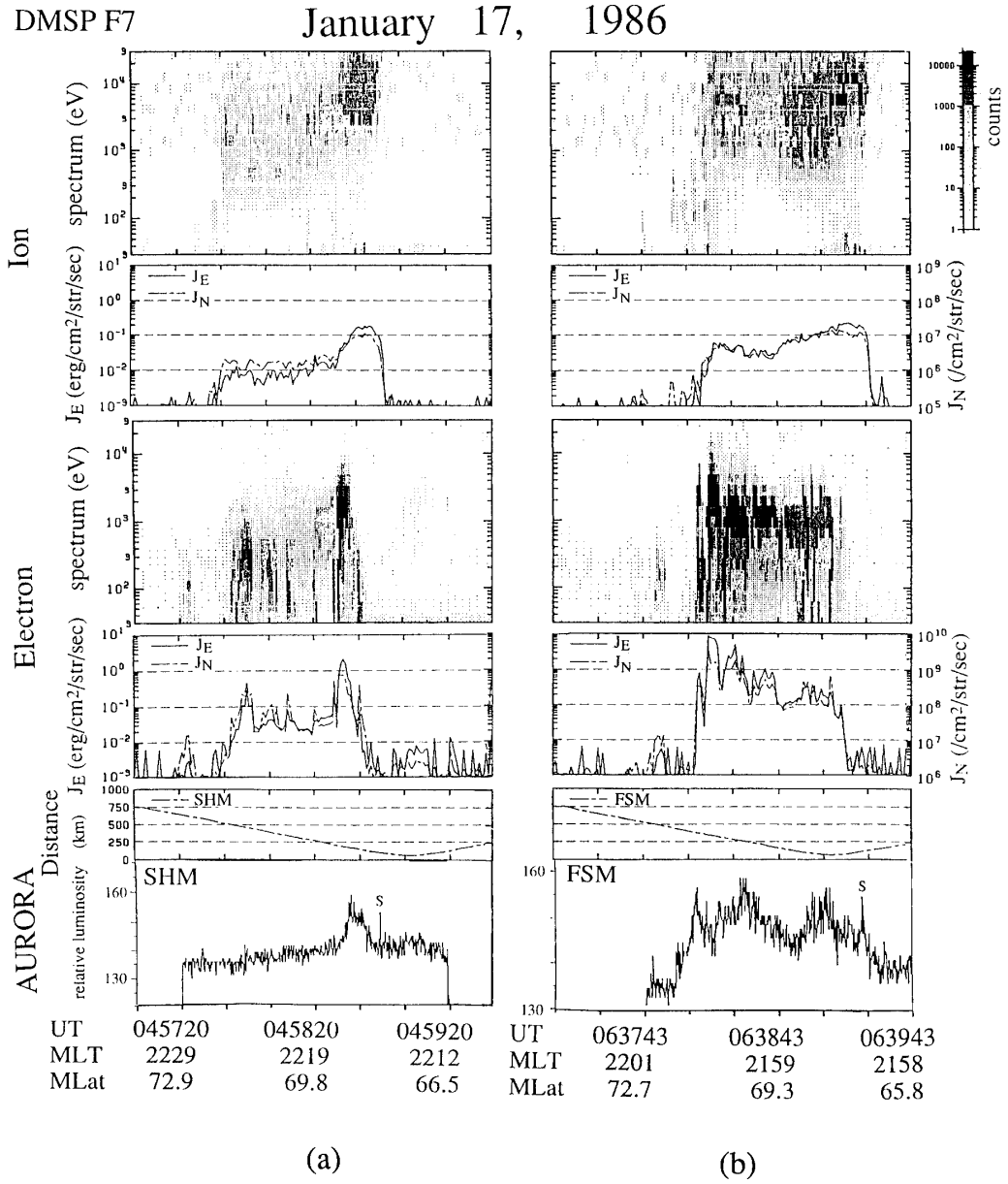

Fig. 2 *Particle data from DMSP F7 and auroral data from the all-sky TV. The top four panels show the spectrums and total flux (J_E for the energy flux and J_N for the number flux) for ions and electrons. The second panel from the bottom shows the distance between the satellite foot point and the zenith of the auroral station calculated at an altitude of 110 km. The bottom panel shows the relative luminosity of the aurora along the DMSP orbit track, which is presented with 256 levels in logarithmic scale. The sharp peak designated with the letter S in the panel is the light from a star. (a) Particle data between 045700UT and 045940UT on January 17, 1986 and auroral data obtained at SHM. (b) Particle data between 063703UT and 063943UT on the same day and auroral data obtained at FSM*

intensification followed by a clear poleward, and somewhat equatorward, expansion started at 0633UT as indicated by the broken line in the plot. This intensification occurred in an auroral arc located poleward of the aurora structure that moved southward during the recovery of the previous event. The intensified aurora expanded beyond 72° by ~0645UT, while diffuse auroral region expanded southward to ~67°. DMSP passed the auroral region during this second major poleward expansion; between 063743UT and 063943UT.

Particle data from DMSP F7 during the period is compared with the all-sky TV auroral data in Fig. 2b. Structured precipitation with several inverted-V, which is a characteristic of BPS, is evident from 063807UT (71.4°) to 063843UT (69.3°). It should be noted that the most intense precipitation occurred in the most poleward inverted-V region with energy flux of 8.6 erg/cm^2/str/sec at 71.2°. The region of multiple inverted-V structures coincides with the region of poleward expanding aurora at FSM as shown in the meridian plot (Fig. 1b). Equatorward boundary of BPS, which indicates the discrete auroral precipitation, was 69.3° for this event. The ion precipitation at the electron BPS region was relatively strong compared to the 0458UT event. It should be also noted that the energy flux tended to increase with latitude and became ~0.06 erg/cm^2/str/sec at maximum, which is quite a different signature compared to the 0458UT event.

The lower latitude electron precipitation until 063912UT (67.6°) shows rather diffuse precipitation with a weak collapsed inverted-V structure. Note that this region coincides with the diffuse auroral region which was formed in association with the southward motion of the discrete aurora during the recovery of the previous auroral activation that started at 0617UT as shown in the meridian plot (Fig. 1b). The collapsed inverted-V like structure, within the CPS precipitation (Fig. 2b) must be therefore associated with the first auroral activation. On the other hand, the ion precipitation at the lower latitude, shows a clear latitudinal dependence in average energy which is more evident than that in the 0458UT event. The average energy tended to become higher until 67.8° (~10 keV in average energy).

3. Discussion and Conclusion

We have shown that the entire precipitation pattern including BPS and CPS both for electron and ion changes significantly with the auroral expansion. Particularly, CPS electron precipitation took place only during the second event after the expansion onset. The electron CPS therefore changes also dynamically and is not in a stable region which merely shifts its latitude as was suggested by WINNINGHAM *et al.* (1975). As shown in Figs. 1b and 2b, the enhanced CPS is closely related to the previous auroral activation and its southward auroral motion. We suggest that the main part of CPS electron precipitation is attributable to newly accelerated electrons at the auroral substorm onset and injected to the inner magnetosphere. This region would expand in latitudinal direction due to the earthward transport of the injected particles, but also due to the transition of the onset region (or acceleration region) relatively poleward of the former expansion.

As for CPS ion precipitation, which is defined as the precipitation equatorward

of the electron BPS, its latitudinal width was increased after the expansion onset mainly due to equatorward shift of its low latitude boundary. NEWELL and MENG (1987) observed an equatorward shift of a dispersionless precipitation boundary for both electrons and protons at the substorm onset and suggested that this would represent the substorm injection boundary (MCILWAIN, 1974). Both events discussed in this study were not directly observed exactly at the onset. We therefore cannot confirm a dispersionless injection boundary in our study. It should be, however, noted that the low latitude boundary of ions was equatorward than that of electrons in our two cases and the ion precipitation did not enhance significantly after the expansion in contrast to drastic enhancement of electron precipitation. Moreover, we observed a permanent structure for the ion in this region where the average energy tends to increase with decreasing latitude, independent of the phase of auroral expansion, which is consistent with an adiabatic compression of the plasma sheet (HARDY *et al.*, 1989). We suggest that the entire structure of CPS ion precipitation would be also controlled by such a mechanism which has a longer time scale than the auroral expansion in addition to the substorm associated injection. Such quite different signature in electron and ion precipitations could be due to the longer bounce period and therefore longer loss time of the ions in the plasma sheet compared to the electrons.

The different behavior of electrons and ions at CPS is crucial when we infer from the precipitation pattern its conjugate area of the onset region in the magnetosphere. We have shown that the expansion of the auroral arc, which was identified from the TV and from the inverted-V electron precipitation, started from the most equatorward edge of electron precipitation. Note that this arc was located at the poleward boundary of the CPS ion precipitation. From the electron observations therefore we may conclude the onset region to be the inner edge of the plasma sheet, while from the ion observations we may conclude the onset region to be at the outer edge of central plasma sheet, provided that CPS ions also are thought to originate from the central plasma sheet in the magnetosphere as was suggested for the electrons (LUI *et al.*, 1977). It is not yet well understood where CPS or BPS maps in the magnetosphere (FELDSTEIN and GALPERIN, 1985). It is necessary to look for a consistent mapping model both for ion and electron.

We have shown that the enhanced BPS electron precipitation associated with substorm (*e.g.*, WINNINGHAM *et al.*, 1975) was clearly accompanied by the enhanced energetic ion precipitation. In accordance with the poleward expansion of aurora, the ion precipitation also became strongest at higher latitude which was collocated at the region of strongest electron precipitation in spite of deceleration of protons along the field line at the inverted-V structure (Fig. 2b). It is therefore inferred that these ions and electrons would be accelerated due to the same mechanism associated with substorm. LYONS *et al.* (1988) reported on general association between the discrete aurora and isotropic ion precipitation and suggested that these ions thread the tail current sheet at distances where ion motion violates the guiding center approximations. Although the mapping is yet an unsolved problem as discussed above, one of the candidate to explain such acceleration would be transient electric fields due to the magnetic field change at the tail current sheet associated

with the onset (HEIKKILA and PELLINEN, 1977).

Development of electron and ion precipitation during auroral expansion is summarized in the illustration of Fig. 3. The figure shows three latitudinal profiles of ion and electron energy flux at three stages of auroral expansions produced by different mechanisms discussed above. The left figure illustrates the observation before poleward expansion onset in Fig. 2a. The electron precipitation is weak at the higher latitude with an auroral arc at its equatorward boundary and without significant CPS precipitation at the lower latitude. There is weak ion precipitation at the latitude of the quiet BPS electron precipitation. The ion precipitation becomes stronger at the latitude of the auroral arc at the equatorward boundary of the BPS and becomes more stronger at the lower latitude which represent the stable convecting ions. The middle figure is for the onset of a poleward expansion deduced from the two observations, before and after the onset. The poleward expansion of the aurora starts from the auroral arc at the quatorward boundary of electron

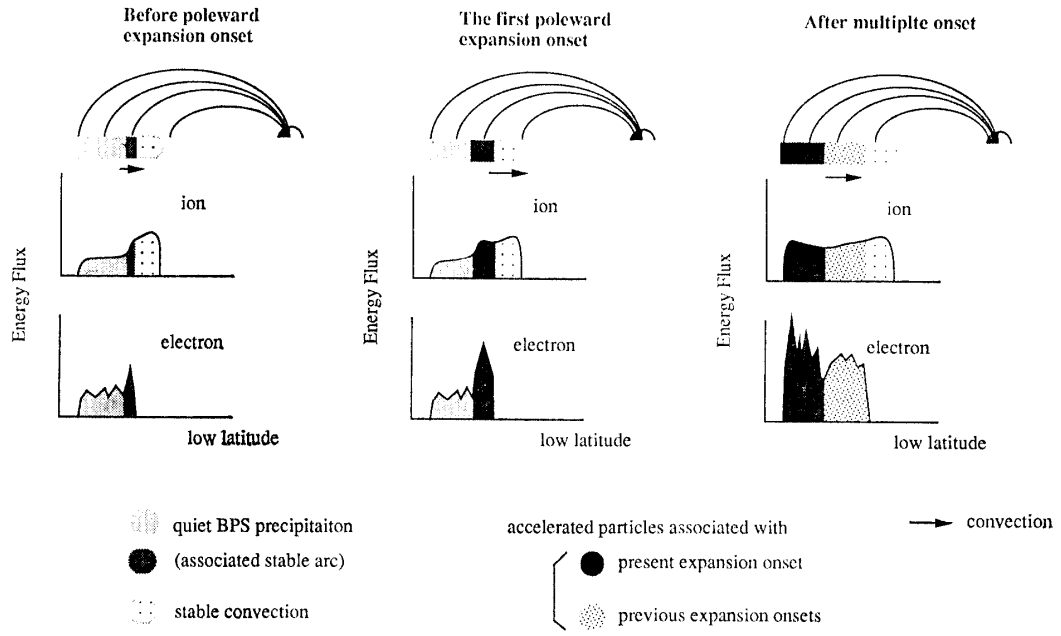

Fig. 3. Illustration of the latitudinal profile of ion and electron energy flux at different stage of auroral expansions and relationships to different acceleration mechanism in the magnetospheric source region. (Figure left) Before poleward expansion onset corresponding to Fig. 2a. Cold ion and electron precipitation at the higher latitude with an auroral arc at its equatorward boundary and no CPS precipitation at the lower latitude. The ion precipitation enhances at the latitude of the auroral arc at the equatorward boundary of the BPS and becomes stronger at the lower latitude which would represent the stable convecting ions. (Figure center) At the onset of poleward expansion deduced from Figs. 2a and 2b. Poleward expansion of the aurora starts from the auroral arc at the equatorward boundary. Associated with this electron precipitation, the ion precipitation is also enhanced. (Figure right) During poleward expansion, after several intensifications corresponding to Fig. 2b. The BPS precipitation is strongest at the poleward part both for electrons and ions associated with the present activation. At the lower latitude of the BPS equatorward boundary, there is a diffuse precipitation region with collapsed inverted-V structure in association with the previous auroral activation.

precipitation as is shown in Fig. 1a. Associated with this precipitation, the ion precipitation is also enhanced. The right figure illustrates the observation during poleward expansion, after several intensifications (Fig. 2b). The BPS precipitation is strongest at the poleward part both for electrons and ions associated with the present activation. At the lower latitude of the BPS equatorward boundary, there is a diffuse precipitation region in association with the injection from the previous auroral activation. The enhanced convection transports electrons and ions earthward (to lower latitude).

Acknowledgments

We are greatly indebted to those members of the Geophysics Research Laboratory, University of Tokyo who were involved in constructing the instruments and collecting the aurora and magnetic data. The DMSP data was provided by WDC-A for Solar Terrestrial Physics through WDC-C2 for Aurora (National Institute for Polar Research). We would like to thank H. NAKAJIMA for his help in constructing computer programs for DMSP data plot. The work of R. NAKAMURA was supported by the Fellowship of the Japan Society for the Promotion of Science.

References

FELDSTEIN, Ya. I. and GALPERIN, Yu. I. (1985): The auroral luminosity structure in the high-latitude upper atmosphere; Its dynamic relationship to the large-scale structure of the Earth's magnetosphere. Rev. Geophys., **23**, 217–275.

FRANK, L. A. and ACKERSON, K. L. (1971): Observations of charged particle precipitation into the auroral zone. J. Geophys. Res., **76**, 3612–3643.

HARDY, D. A., SCHMITT, L. K., GUSSENHOVEN, M. S., MARSHALL, F. J., YEH, H. C., SHUMAKER, T. L., HUBE, A. and PANTAZIS, J. (1984): Precipitating electron and ion detectors (SSJ/4) for the block 5D/flights 6–10 DMSP satellites; Calibration and data presentation. Rep. AFGL-TR-84-0317, Bedford, Mass. Air Force Geophys. Lab., Hanscom Air Force Base.

HARDY, D. A., GUSSENHOVEN, M. S. and BRAUTIGAM, D. (1989): A statistical model of auroral ion precipitation. J. Geophys. Res., **94**, 370–392.

HEIKKILA, W. J. and PELLINEN, R. J. (1977): Localized induced electric field within the magnetotail. J. Geophys. Res., **82**, 1610–1616.

LUI, A. T. Y. and ANGER, C. D. (1973): A uniform diffuse aurora emission seen by the Isis-2 scanning photometer. Planet. Space Sci., **21**, 799–809.

LUI, A. T. Y., VENKATESAN, D., ANGER, C. D., AKASOFU, S.-I., HEIKKILA, W. J., WINNINGHAM, J. D. and BURROWS, J. R. (1977): Simultaneous observations of particle precipitation and auroral emissions by the ISIS 2 satellite in the 19–24 MLT sector. J. Geophys. Res., **82**, 2210–2226.

LYONS, L. R. and EVANS, D. S. (1984): An association between discrete aurora and energetic particle boundaries. J. Geophys. Res., **89**, 2395–2400.

LYONS, L. R., FENNELL, J. F. and VAMPOLA, A. L. (1988): A general association between discrete aurora and ion precipitation from the tail. J. Geophys. Res., **93**, 12932–12940.

MCILWAIN, C. E. (1974): Substorm injection boundaries. Magnetospheric Physics, ed. by B. M. MCCORMAC, Hingham, Mass., D. Reidel, 143–154.

NEWELL, P. T. and MENG, C.-I. (1987): Low altitude observations of dispersionless substorm plasma injections. J. Geophys. Res., **92**, 10063–10072.

OGUTI, T., KITAMURA, T. and WATANABE, T. (1988): Global aurora dynamics campaign, 1985–1986. J. Geomag. Geoelectr., **40**, 485–504.

WINNINGHAM, J. D., YASUHARA, F., AKASOFU, S.-I. and HEIKKILA, W. J. (1975): The latitudinal morphology of 10-eV to 10-keV electron fluxes during magnetically quiet and disturbed times in the 2100–0300 MLT sector. J. Geophys. Res., **80**, 3148–3171.

(*Received June 8, 1991; Revised manuscript received September 24, 1991*)